PHYSICAL REVIEW B **95**, 161301(R) (2017)

Phase diagram of boron-doped diamond revisited by thickness-dependent transport studies

J. Bousquet,[1,2] T. Klein,[1,2] M. Solana,[1,2] L. Saminadayar,[1,2] C. Marcenat,[3,4] and E. Bustarret[1,2]
[1]*Université Grenoble Alpes, Institut NEEL, F-38042 Grenoble, France*
[2]*CNRS, Institut NEEL, F-38042 Grenoble, France*
[3]*Université Grenoble Alpes, INAC-SPSMS, F-38000, France*
[4]*CEA, INAC-Pheliqs, F-38000, France*

(Received 24 July 2016; revised manuscript received 2 March 2017; published 10 April 2017)

We report on a detailed study of the electronic properties of a series of boron-doped diamond epilayers with dopant concentration ranging from 1×10^{20} to 3×10^{21} cm^{-3} and thicknesses ($d_\perp$) ranging from 2 μm to 8 nm. By using well-defined mesa patterns that minimize the parasitic currents induced by doping inhomogeneities, we have been able to unveil a new phase diagram differing from all previous reports. We first show that the boron concentration corresponding to the onset of superconductivity (above 50 mK) does not coincide with that of the metal-insulator transition; the latter one corresponding to the vanishing of the residual conductivity σ_0 (deduced from $\sigma(T) = \sigma(0) + A\sqrt{T}$ fits to the low temperature data). Moreover, a dimensional crossover from 3D to 2D transport properties could be induced by reducing $d_\perp$ in both (metallic) nonsuperconducting and superconducting epilayers but without any reduction of T_c in the latter.

DOI: 10.1103/PhysRevB.95.161301

The discovery of superconductivity in boron-doped diamond was first reported in 2004 by Ekimov *et al.* [1] in high-pressure, high-temperature polycrystalline samples and was rapidly confirmed in both polycrystalline films [2] and (100)-oriented epilayers [3] grown by microwave plasma enhanced chemical vapor deposition (MPCVD). Various experimental works including (i) the softening and broadening of the Brillouin zone center phonon mode at T_c [4], (ii) the existence of an isotopic effect on T_c [5], or (iii) the observation of a fully open superconducting gap (Δ) with $2\Delta(0)/k_B T_c$ being close to the standard BCS weak coupling value [6] then provided strong experimental insights in favor of a standard electron-phonon coupling mechanism. With critical temperatures (T_c) rising up to ~10 K [7,8] despite very small carrier concentrations (~10^{21} cm^{-3}), this discovery revived the interest for "superconducting semiconductors" as promising candidates for possible new, conventional, high-T_c superconductors (for a review, see Refs. [9,10]).

Moreover, early studies [7,11] suggested that T_c remains surprisingly large down to the metal-insulator transition (MIT) suggesting that the boron concentration (n_B) corresponding to the onset of superconductivity (n_c^S) coincides with that of the MIT : $n_c^{\mathrm{MIT}} \sim n_c^S \sim 4$–$5 \times 10^{21}$ cm^{-3}. However, it has been suggested that T_c scales as $T_c \propto (n_B/n_c^{\mathrm{MIT}} - 1)^{1/2}$ [11] in striking contrast with the exponential dependence expected from the standard McMillan expression, and that T_c strongly—and anomalously—depends on the thickness of the epilayers [12]. Finally, a sharp peak in the resistivity prior to the superconducting transition has been reported in granular films and interpreted as a signature of a metal-bosonic insulator-superconductor transition [13]. All those measurements are indicating that this system is an interesting platform to study the interaction between electronic correlations, disorder and superconductivity in the vicinity of the—still highly debated—insulator-superconductor transition (for a review, see Ref. [14]).

We present here a detailed study of the electronic properties of boron-doped diamond epilayers in the vicinity of the MIT. Both the influence of the doping content and of the epilayer thickness ($d_\perp$) has been revisited. The main breakthrough of our work is the use of well defined mesa patterns (see Fig. 1) that enabled us to control the current distribution within the sample, and hence to minimize the effects associated to parasitic current paths induced by doping inhomogeneities. As previously reported in C:B films (see Refs. [11,15] and references therein), the temperature dependence of the normal state conductivity, $\sigma(T)$, can be well described by quantum interference effects (weak localization and/or electron-electron interactions) for $n_B \geqslant n_c^{\mathrm{MIT}} \sim 3 \pm 1 \times 10^{20}$ cm^{-3}. However, in striking contrast with all previous reports, we did not observe any superconducting transition down to ~50 mK for $n_B \leqslant n_c^S = 11 \pm 2 \times 10^{20}$ cm^{-3}, unveiling the existence of a nonsuperconducting phase for $n_c^{\mathrm{MIT}} \leqslant n_B \leqslant n_c^S$.

Moreover, whereas $\sigma(T)$ can be well described by a 3D $\sigma_0 + AT^{1/2}$ law down to the lowest temperature (below ~5 K) in the thickest samples, a logarithmic divergence of the resistivity (characteristic of 2D quantum corrections) has been observed in the thinnest samples. However, despite this dimensional crossover, we did not observe any reduction of T_c with the sample thickness down to 8 nm (for $n_B > n_c^S$) and we hence show that superconductivity can be observed in both 3D and 2D electronic regimes.

A series of boron-doped epilayers was grown by MPCVD on top of hundred-nanometer-thick nonintentionally doped (NID) layers deposited on IIa- or Ib-type [100]-oriented diamond substrates. The total pressure in the vertical silica tube reaction chamber was set to 33 or 50 torr in order to stabilize the sample temperature to ~910 °C and ~830 °C during the growth of an NID and a doped layer, respectively. After a first exposure of the substrate to a pure hydrogen plasma, methane ($CH_4/H_2 = 1\%$ molar ratio) has been added for the buffer layer deposition. The gas mixture has been complemented by addition of oxygen $CH_4/O_2/H_2$ (0.75%, 0.25%) to reduce the residual boron incorporation and the surface roughness [16]. Finally, gas mixtures with various concentrations of diborane were used for the B-doped epilayers. The substrate was placed either within or at the vicinity of the plasma ball and the growth parameters corresponding to these two positions

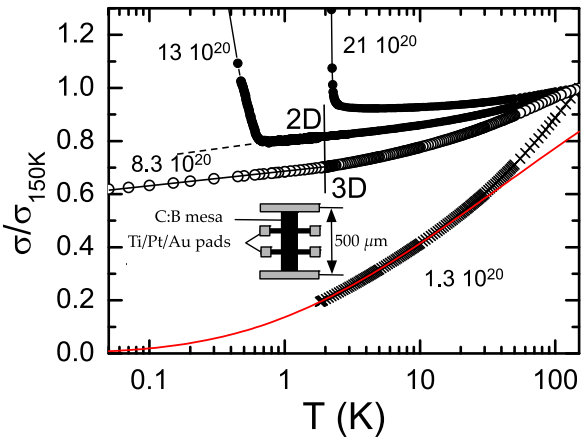

FIG. 1. Temperature dependence of the conductivity (renormalized to its value at 150 K) in four boron-doped diamond epilayers for the indicated carrier concentration (in cm^{-3}). As shown, both superconducting (solid circles), metallic nonsuperconducting (open circles), and insulating (crosses) samples can be obtained depending on the boron concentration. For the lowest doping, a very reasonable fit to the data can be obtained (red solid line) using Mott's law in the variable range hoping limit $[\sigma(T) \propto \exp(-(T_0/T)^{0.25}]$ in agreement with previous measurements [11]. A dimensional crossover separating 3D and 2D interaction regimes (vertical line) has been observed in the thinnest samples. The two black lines show the typical logarithmic dependence of the conductivity in the 2D regime (see Fig. 4 and text for details). (Inset) Sketch of the mesa structured Hall bars patterned on the 3×3 mm^2 epilayers.

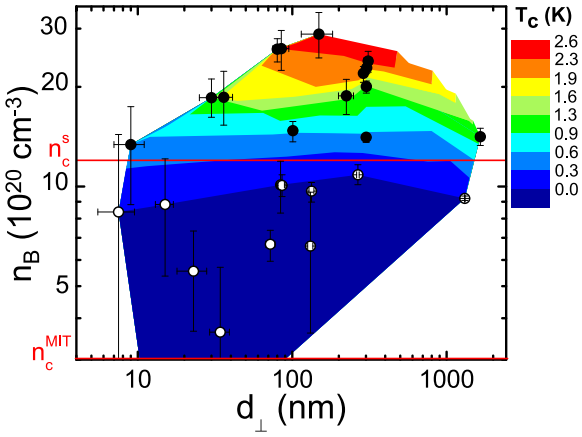

FIG. 2. Critical temperature as a function of thickness ($d_\perp$) and doping content (n_B, deduced from Hall effect measurements) in C:B epilayers. A nonsuperconducting metallic phase (open symbols) has been observed for $n_c^{MIT} < n_B < n_c^S$ (with $n_c^{MIT} = 3 \pm 1 \times 10^{20}$ cm^{-3} and $n_c^S = 1.1 \pm 0.2 \times 10^{21}$ cm^{-3}). This color plot clearly indicates that T_c does not depend on the layer thickness (down to 8 nm). Note that 2D-like quantum interference effects have been observed in the thinnest samples [see, for instance, Figs. 4(c) and 4(d)] showing that superconductivity can be obtained in both 3D- and 2D-like samples. Insulating layers obtained for $n_B \leqslant n_c^{MIT}$ have not been reported.

are summarized in Table I. The thickness of the epilayers was controlled by varying the growth time and checked by ellipsometric measurements [17]. A total number of 26 samples, with doping level $1 \times 10^{20} \leqslant n_B \leqslant 3 \times 10^{21}$ cm^{-3} and thickness 8 nm $\leqslant d_\perp \leqslant 2\,\mu$m were grown.

Transport measurements have been performed between 300 and 3 K using a Quantum Design Physical Properties Measurements System and down to 50 mK by adding a homemade adiabatic demagnetization refrigeration stage on the former setup and/or by using a standard dilution fridge. Four contact measurements have been carried out on each epilayer first using only silver pasted top contacts (similar to previous studies [11]) and subsequently using well-controlled mesa patterned Hall bars (see sketch in the inset of Fig. 1) delineated from the surrounding doped layers by using O_2 plasma treatment (with Ti/Pt/Au metallic pads). It is important to note that the boron concentrations discussed throughout this work have been deduced from Hall effect measurements

TABLE I. Total gas flow rate, CH_4/H_2 molar ratio, growth rate (in nm/min), and boron to carbon concentration ratio used during the growth process of the epilayers. The substrate was placed either within the plasma ball (position 1) or at its vicinity (position 2).

position	flow rate sccm	CH_4/H_2 %	growth rate nm/min	B/C ppm
1	100 to 400	4	~32	400 to 2500
2	2000	0.5	~5	6000 to 12000

performed on those mesa patterned Hall bars. Even though anomalously small Hall coefficients have been previously reported [7,11] (hindering any reliable determination of the doping concentration from these measurements), the hole concentrations deduced from our measurements performed on mesa patterned geometries are fully consistent with those deduced from ellipsometry measurements [17] and with the boron content determined by secondary ion mass spectroscopy measurements (see [11] for details) performed on selected samples. Note that we have also obtained significantly reduced Hall coefficients when measuring the Hall effect with contacts directly deposited on the top of the samples without further mesa patterning, hence clearly stressing out the necessity of a systematic delineation of the current paths in order to obtain relevant results.

The temperature dependence of the renormalized conductivity of selected characteristic layers, measured on the mesa patterns, are reported Fig. 1. The sample with boron concentration $n_B \leqslant n_c^{MIT} \sim 3 \pm 1 \times 10^{20}$ cm^{-3} displayed an insulating behavior with an exponentially diverging resistivity (see crosses in Fig. 1 for $n_B = 1.3 \times 10^{20}$ cm^{-3}). This temperature dependence was fully consistent with that previously obtained in Ref. [11] and is hence not discussed in further details here. The first result of our study is that no superconducting transition could be observed down to 50 mK after mesa patterning, for $n_B \leqslant n_c^S = 11 \pm 2 \times 10^{20}$ cm^{-3} (see open circles in Fig. 1), in striking contrast with all previous results which were suggesting that the onset of superconductivity coincides with the MIT [7,11]. The concentration and thickness dependence of the critical temperatures, defined as the temperature at which the resistivity decreases to 90% of the normal state value, is displayed in Fig. 2. As shown [see also Fig. 3(b)], T_c vanishes for $n_B \leqslant n_c^S = 11 \pm 2 \times 10^{20}$ cm^{-3}

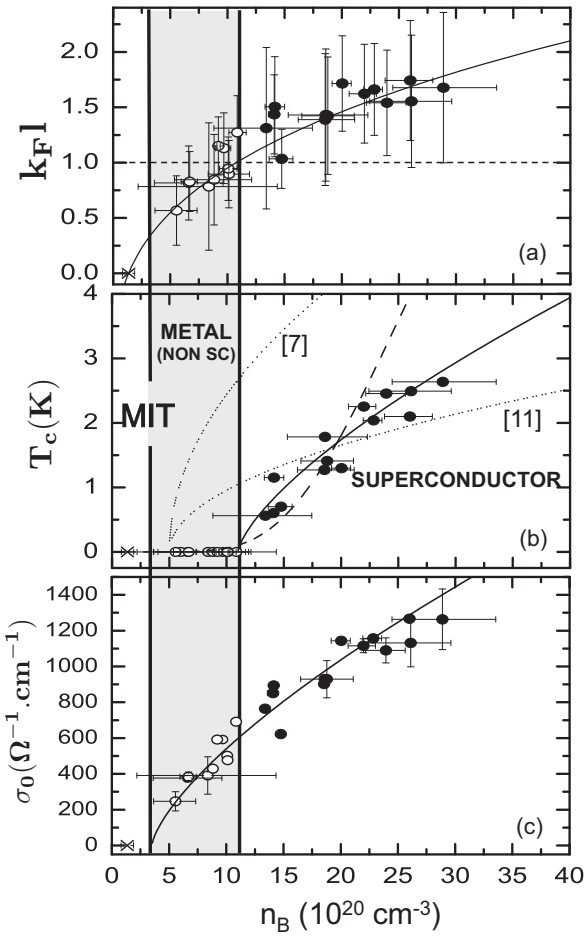

FIG. 3. $k_F l$ value (a), critical temperature (b), and residual conductivity (c) as a function of boron doping in C:B epilayers. The dotted lines in (b) represent the doping dependence previously reported in Refs. [7] and [11] and the dashed line corresponds to the standard MacMillan dependence, introducing the electron-phonon coupling constants deduced from *ab initio* calculations and taking $\mu^* \sim 0.04$. The solid lines are guides to the eyes showing that the MIT transition (vanishing of σ_0) does not coincide with the onset of superconductivity.

whereas the residual resistivity σ_0 deduced from $\sigma(T) = \sigma(0) + A\sqrt{T}$ fits to the low-temperature data only vanishes for $n_B \leqslant n_c^{\mathrm{MIT}} = 3 \pm 1 \times 10^{20}$ cm^{-3} [see Fig. 3(c) and discussion below]. Our data hence clearly indicate the presence of a metallic but nonsuperconducting phase for $n_c^{\mathrm{MIT}} \leqslant n_B \leqslant n_c^S$. Note that, although not previously observed in C:B, a metallic phase separating the insulating from the superconducting one has also been reported in some disordered systems (see, for instance, Ref. [18] and discussion in Ref. [14]).

It is worth noting that the nonsuperconducting metallic phase could not be observed when measuring the resistivity of the same films with pasted silver pads without further mesa-patterning (as done in [11]). On several films, twelve Hall bars have been patterned all over the surface in order to map the distribution of the electronic properties. For $n_B \lesssim n_c^S$, this mapping procedure revealed the presence of incomplete transitions in some of the Hall bars located close to the sample edges, suggesting the presence of percolation paths with larger boron concentrations within the peripheral area. Finally, note also that the T_c values reported here (and in Ref. [11]) are significantly lower than those obtained in Refs. [7,12], the origin of this difference remains unclear.

Let us now switch to the electronic properties of the normal state. The room-temperature mobility of all samples was found to be on the order of $\sim$3 cm^2 V^{-1}s^{-1}, corresponding to conductivities (σ_{RT}) varying between 200 and 2000 Ω^{-1} cm^{-1} for $3 \times 10^{20} \leqslant n_B \leqslant 30 \times 10^{20}$ cm^{-3}. The Ioffe-Regel parameter $k_F l \sim R_Q \sigma_{RT} / n_B^{0.33}$ is then on the order of 1–2 [see Fig. 3(a)], clearly indicating that disorder plays a significant role in the electronic properties (introducing $R_Q = h/e^2 \sim 25$ kΩ). As expected, quantum corrections to the Drude resistivity then show up at low temperature and, as previously reported [11,19], the temperature dependence of all metallic samples can be well described by a $\sigma(T) = \sigma_0 + A\sqrt{T} + BT^p$ [20] law for $5 \lesssim T \lesssim 50$ K. In this temperature range, inelastic scattering is expected to be dominated by electron-phonon interactions and $p = 2$ or 1 depending on the influence of static impurities such as heavy impurities, defects or grain boundaries (see for instance discussion in Ref. [21]). Very reasonable fits to the data could be obtained taking $p \sim 1$–1.5 [see for instance solid (red) lines in Figs. 4(b) and 4(d) for $p = 1$ in $d_\perp \sim 85$ and $\sim$8 nm epilayers]. We obtained $B \sim 0.5 \pm 0.1\ \Omega^{-1}\,\mathrm{cm}^{-1}\,\mathrm{K}^{-1}$ (taking $p = 1$) in all measured samples and the inelastic scattering time τ_Φ is hence scaling as $1/\tau_\Phi \sim [\pi R_Q B]^2 D T^2 \sim [2 \times 10^9\ \mathrm{cm}^{-2}\,\mathrm{K}^{-2}] D T^2$ (D being the diffusion constant $\sim$1–10 cm^2/s). Such a DT^2 scaling of the electron-phonon inelastic scattering rate has been previously reported in disordered systems [22] but a pertinent theoretical model for this dependence is still lacking (see discussion in Ref. [22]). Note that a significantly larger τ_Φ (but with the same $1/T^2$ dependence) has been recently derived from terahertz (THz) absorption measurements in the superconducting state of similar epilayers [21] but the origin of this discrepancy still has to be clarified.

Below $\sim$5 K, in *thick* samples, the temperature dependence is dominated by the $\sqrt{T}$ term and a $\sigma(T) = \sigma_0 + A\sqrt{T}$ law holds down to the lowest temperatures [for $n_B \leqslant n_c^S$, see Fig. 4(a)]. Such a temperature dependence is expected for electron-electron interactions in 3D samples but a change in the p exponent (weak localisation term) can not be excluded [23]. In both cases this $\sqrt{T}$ dependence is characteristic of *3D* samples and, as shown in Figs. 4(c) and 4(d), the temperature dependence can be better described by a $\sigma \propto \ln T$ term for $T \lesssim 2$ K in the *thinnest* samples [see Figs. 1 and 4(c) for $d_\perp \sim 8$ nm]. This logarithmic dependence is, on the contrary, characteristic of quantum corrections in 2D materials (either weak localisation or electron-electron interactions). This 2D behavior is expected to be observed if the thermal coherence length (for electron-electron interactions) and/or diffusion length (for weak localisation effects) $L(T)$ becomes larger than $d_\perp$. Writing $\Delta\sigma \sim 1/[\pi R_Q L(T)]$, one obtains $L(T) \sim 1/[\pi R_Q A\sqrt{T}] \sim 20[\mathrm{nm}]/\sqrt{T}$ ($A \sim 6 \pm 2\,\Omega^{-1}\mathrm{cm}^{-1}\,\mathrm{K}^{-1/2}$ in all measured samples) and a dimensional crossover is expected to be reached for $L(T) \sim d_\perp$, i.e., for $T = T_{cr} \sim 5$ K in the $d_\perp = 8$ nm sample, in very reasonable agreement with the observed behavior.

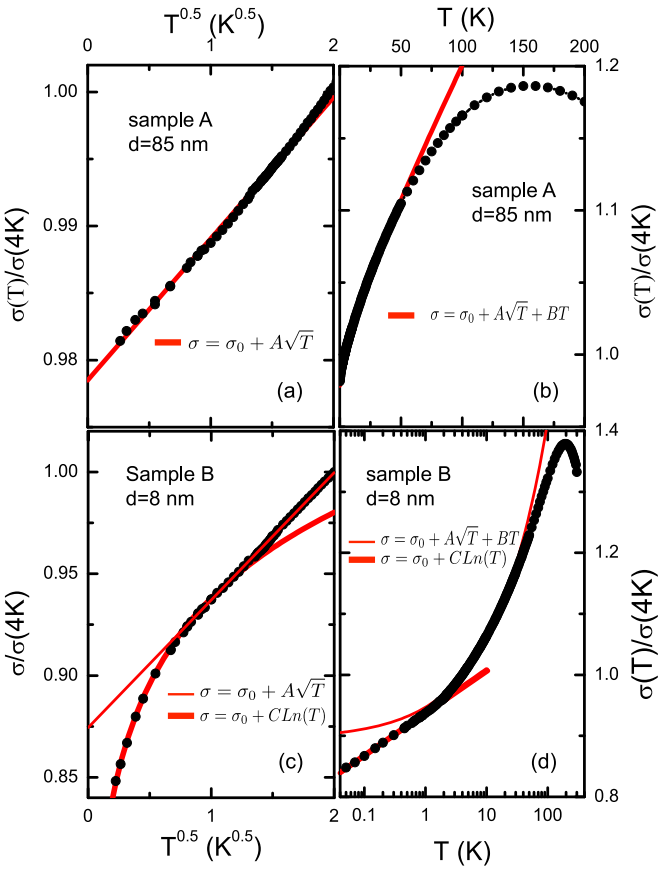

FIG. 4. Temperature dependence of the conductivity for two C:B samples with $n_B \sim 1 \times 10^{21}$ cm^{-3} and $d_\perp \sim 85$ nm (sample A, panel a and b) and $d_\perp \sim 8$ nm [sample B, (c) and (d)]. As shown, for $d_\perp \sim 85$ nm, $\sigma(T)$ can be well described by a $\sigma_0 + A\sqrt{T}$ law [thick solid (red) line in (a)] as expected for 3D electron-electron interaction effects. At higher temperature, weak localization effects have to be taken into account and $\sigma(T) = \sigma_0 + A\sqrt{T} + BT$ [solid (red) line in (b), finally a standard metallic behavior is recovered above ~150 K]. For $d_\perp \sim 8$ nm, $\sigma(T)$ is better described by a ln$T$ term (thick (red) lines in panel c and d) than by a $\sqrt{T}$ term [thin (red) lines in (c) and (d)], as expected in the 2D limit.

The second important point of this study is that superconductivity is observed in both 2D and 3D interaction regimes (see Fig. 1), clearly showing that superconductivity is robust to this dimensional crossover. Indeed, as shown in Fig. 2, we did not observe any significant decrease of the critical temperature with $d_\perp$, in striking contrast with the clear decrease of T_c reported in Ref. [12]. It is important to note that the 2D behavior here refers to the quantum corrections to the normal state electronic properties. Interaction effects are also expected to lead to a reduction of T_c in thin samples [24] but this effect is only expected to be important for $l \ll d_\perp$ (l being the mean free path). Indeed, for $R_\square/[\pi R_Q] \ll 1$, one expects $\Delta T_c/T_{c,0} \approx -R_\square/R_c$ where $R_\square$ is the square resistance, $R_c = 6R_Q/\gamma^3$, $e^\gamma = [\hbar/\tau^*]/[k_B T_{c,0}]$ and $\tau^* = \max\{\tau, \tau(d_\perp/l)^2\}$ [25] and, as $d_\perp \gg l \sim 4$Å, $\gamma \to 1$ ($\tau \sim 10^{-15}$ s) so that no significant reduction of T_c due to interaction effects is expected in our case.

The new phase diagram is displayed in Fig. 3. As shown, superconductivity vanishes for $k_F l \sim 1$ suggesting that disorder might play a significant role. In this regime, disorder is expected to hinder the formation of long range phase coherence and localised Cooper pairs could then be preformed in an exotic insulting phase characterised by a small but hard gap (see Ref. [26] and discussion therein). However, it has been shown [27] that $k_F l$ is not necessarily a good parameter to characterize disorder when superconductivity is concerned as the effect of doping (weakening of the BCS potential by decreasing the carrier concentration) can be much larger on T_c than that of increasing the disorder. In C:B, *ab initio* calculations [28,29] suggested that the electron-phonon coupling constant is on the order of $\lambda_{\text{e-ph}} \sim 0.2$–$0.25$ in this doping range and the observed rapid increase of T_c for $n_B \sim 2n_c^{\text{MIT}}$ is consistent with the exponential increase expected by the standard McMillan expression, assuming, however, a reduced μ^* value [~0.04, see dashed line in Fig. 3(b)].

In conclusion, we have revisited the phase diagram of boron doped diamond epilayers. A new diagram has been obtained by using mesa patterns that minimize the parasitic currents induced by doping inhomogeneities. This well-defined geometry enabled us to unveil the presence of a metallic, nonsuperconducting phase for $n_c^{\text{MIT}} \leqslant n_B \leqslant n_c^S$, with $n_c^{\text{MIT}} = 3 \pm 1 \times 10^{20}$ cm^{-3} and $n_c^S = 11 \pm 2 \times 10^{20}$ cm^{-3}. Finally, we have demonstrated that the critical temperature is not affected by the epilayer thickness (down to 8 nm) even though the low-temperature normal state resistivity clearly indicates a crossover from a $\sqrt{T}$ (3D) to a ln T (2D) dependence in the thinnest samples.

The authors would like to thank T. Crozes, S. Dufresnes, B. Fernandez, T. Fournier, and G. Julie from the Nanofab platform (Grenoble, France) for their help during the samples contacts preparation.

[1] E. A. Ekimov, V. A. Sidorov, E. D. Bauer, N. N. Mel'nik, N. J. Curro, J. D. Thompson, and S. M. Stishov, Nature (London) **428**, 542 (2004).

[2] Y. Takano, M. Nagao, I. Sakaguchi, M. Tachiki, T. Hatano, K. Kobayashi, H. Umezawa, and H. Kawarada, Appl. Phys. Lett. **85**, 2851 (2004).

[3] E. Bustarret, J. Kacmarcik, C. Marcenat, E. Gheeraert, C. Cytermann, J. Marcus, and T. Klein, Phys. Rev. Lett. **93**, 237005 (2004).

[4] E. A. Ekimov, V. A. Sidorov, A. V. Rakhmanina, N. N. Mel'nik, R. A. Sadykov, and J. D. Thompson, Sci. Technol. Adv. Mater. **7**, S2 (2006); M. Hoesch, T. Fukuda, J. Mizuki, T. Takenouchi, H. Kawarada, J. P. Sutter, S. Tsutsui, A. Q. R. Baron, M. Nagao, and Y. Takano, Phys. Rev. B **75**, 140508 (2007).

[5] N. Dubrovinskaia, L. Dubrovinsky, T. Papageorgiou, A. Bosak, M. Krisch, H. F. Braun, and J. Wosnitza, Appl. Phys. Lett. **92**, 132506 (2008); E. A. Ekimov, V. A. Sidorov, A. V. Zoteev, J. B. Lebed, J. D. Thompson, and S. M. Stishov, Sci. Technol. Adv. Mater. **9**, 044210 (2008); P. Achatz, F. Omnès, L. Ortéga, C. Marcenat, J. Vacík, V. Hnatowicz, U. Köster, F. Jomard and E. Bustarret, Diam. Rel. Mat. **19**, 814 (2010).

[6] B. Sacépé, C. Chapelier, C. Marcenat, J. Kacmarcik, T. Klein, M. Bernard, and E. Bustarret, Phys. Rev. Lett. **96**, 097006 (2006); K. Ishizaka, R. Eguchi, S. Tsuda, T. Yokoya, A. Chainani, T. Kiss, T. Shimojima, T. Togashi, S. Watanabe, C.-T. Chen, C. Q. Zhang, Y. Takano, M. Nagao, I. Sakaguchi, T. Takenouchi, H. Kawarada, and S. Shin, *ibid.* **98**, 047003 (2007); J. Kacmarcik, C. Marcenat, C. Cytermann, A. Ferreira da Silva, L. Ortega, F. Gustafsson, J. Marcus, T. Klein, E. Gheeraert, and Etienne Bustarret, Physica Status Solidi (a) **202**, 2160 (2005); M. Ortolani, S. Lupi, L. Baldassarre, U. Schade, P. Calvani, Y. Takano, M. Nagao, T. Takenouchi, and H. Kawarada, Phys. Rev. Lett. **97**, 097002 (2006).

[7] A. Kawano, H. Ishiwata, S. Iriyama, R. Okada, T. Yamaguchi, Y. Takano, and H. Kawarada, Phys. Rev. B **82**, 085318 (2010).

[8] H. Okazaki, T. Wakita, T. Muro, T. Nakamura, Y. Muraoka, T. Yokoya, S.-I. Kurihara, H. Kawarada, T. Oguchi, and Y. Takano, Appl. Phys. Lett. **106**, 052601 (2015).

[9] X. Blase, E. Bustarret, C. Chapelier, T. Klein, and C. Marcenat, Nat. Mater. **8**, 375 (2009)

[10] E. Bustarret, Physica C **514**, 36 (2015).

[11] T. Klein, P. Achatz, J. Kacmarcik, C. Marcenat, F. Gustafsson, J. Marcus, E. Bustarret, J. Pernot, F. Omnes, B. E. Sernelius, C. Persson, A. Ferreira da Silva, and C. Cytermann, Phys. Rev. B **75**, 165313 (2007).

[12] S. Kitagoh, R. Okada, A. Kawano, M. Watanabe, Y. Takano, T. Yamaguchi, T. Chikyow, and H. Kawarada, Physica C **470**, S610 (2010).

[13] G. Zhang, M. Zeleznik, J. Vanacken, P. W. May, and V. V. Moshchalkov, Phys. Rev. Lett. **110**, 077001 (2013).

[14] Y.-H. Lin, J. Nelson, A. M. Goldman, Physica C **514**, 130 (2015); V. F. Gantmakher and V. T. Dolgopolov, Phys.-Usp. **53**, 49 (2010).

[15] E. Bustarret, P. Achatz, B. Sacépé, C. Chapelier, L. Oetega, and T. Klein, Phil. Trans. R. Soc. A **366**, 267 (2008).

[16] A. B. Harker, J. Mater. Res. **5**, 818 (1990).

[17] J. Bousquet, G. Chicot, D. Eon, and E. Bustarret, Appl. Phys. Lett. **104**, 021905 (2014).

[18] See, for instance, D. J. Bishop, E. G. Spencer, and R. C. Dynes, Solid State Electron. **28**, 73 (1985); N. Mason and A. Kapitulnik, Phys. Rev. B **64**, 060504(R) (2001).

[19] G. Chicot, A. Fiori, N. Volpe, T. N. Tran Thi, J. C. Gerbedoen, J. Bousquet, M. P. Alegre, J. C. Piñero, D. Araujo, F. Jomard, A. Soltani, J. C. De Jaeger, J. Morse, J. Härtwig, N. Tranchant, C. Mer-Calfati, J. C. Arnault, J. Delahaye, T. Grenet, D. Eon, F. Omnes, J. Pernot, and E. Bustarret, J. Appl. Phys. **116**, 083702 (2014).

[20] B. L. Altshuler and A. G. Aronov, *Electron-Electron Interaction in Disordered Conductors*, edited by A. L. Efros and M. Pollak (Elsevier, Amsterdam, 1985).

[21] A. Kardakova, A. Shishkin, A. Semenov, G. N. Goltsman, S. Ryabchun, T. M. Klapwijk, J. Bousquet, D. Eon, B. Sacépé, Th. Klein, and E. Bustarret, Phys. Rev. B **93**, 064506 (2016).

[22] A. K. Meikap, Y. Y. Chen, and J. J. Lin, Phys. Rev. B **69**, 212202 (2004); Y. L. Zhong and J. J. Lin, Phys. Rev. Lett. **80**, 588 (1998).

[23] A detailed study of the field dependence of the conductivity would be required to distinguish between those two scenarios but such a study is beyond the scope of the present paper, see for instance T. Klein, O. G. Symko, and C. Paulsen, Phys. Rev. B **51**, 12805 (1995) and references therein.

[24] H. Fukuyama, Physica B+C **126**, 306 (1984); A. M. Finkel'stein, Physica B **197**, 636 (1994).

[25] M. A. Skvortsov and M. V. Feigel'man, Phys. Rev. Lett. **95**, 057002 (2005).

[26] M. V. Feigel'man, L. B. Ioffe, V. E. Kravtsov, and E. A. Yuzbashyan, Phys. Rev. Lett. **98**, 027001 (2007).

[27] U. Givan and Z. Ovadyahu, Phys. Rev. B **86**, 165101 (2012).

[28] Y. Ma, J. S. Tse, T. Cui, D. D. Klug, L. Zhang, Y. Xie, Y. Niu, and G. Zou, Phys. Rev. B **72**, 014306 (2005); L. Boeri, J. Kortus, and O. K. Andersen, Phys. Rev. Lett. **93**, 237002 (2004); K. Kadas, L. Vitos, and R. Ahuja, Appl. Phys. Lett. **92**, 052505 (2008).

[29] H. J. Xiang, Z. Li, J. Yang, J. G. Hou, and Q. Zhu, Phys. Rev. B **70**, 212504 (2004); X. Blase, Ch. Adessi, and D. Connétable, Phys. Rev. Lett. **93**, 237004 (2004).